# Lawrence Berkeley National Laboratory
**LBL Publications**

**Title**
Probing quantum confinement of single-walled carbon nanotubes by resonant soft-x-ray emission spectroscopy

**Permalink**
https://escholarship.org/uc/item/3zt164pq

**Authors**
Zhong, Jun
Chiou, Jauwern
Dong, Chunli
et al.

**Publication Date**
2008-08-15

# Probing quantum confinement of single-walled carbon nanotubes by resonant soft-x-ray emission spectroscopy

Jun Zhong[a,b], Jauwern Chiou[b,e], Chunli Dong[b,f], Li Song[c], Chang Liu[d], Sishen Xie[c], Huiming Cheng[d], Way-Faung Pong[e], Chinglin Chang[e], Yangyuan Chen[f], Ziyu Wu[a*], Jinghua Guo[b*]

[a] Institute of High Energy Physics, Chinese Academy of Sciences, Beijing 100049

[b] Advanced Light Source, Lawrence Berkeley National Laboratory, Berkeley, CA 94720

[c] Institute of Physics, Chinese Academy of Sciences, Beijing 100080

[d] Institute of Metal Research, Chinese Academy of Sciences, Shenyang 110015

[e] Department of Physics, Tamkang University, Tamsui, Taiwan 251

[f] Institute of Physics, Taipei, Taiwan 115

**Abstract:**

We report the band-structure changes near Fermi level for single-walled carbon nanotubes (SWNTs) with diameters down to 1 nm from the study of soft-x-ray absorption and resonant emission spectroscopy. The observed quantum confinement of SWNTs affects both $\pi$ and $\sigma$ bands and bandgap through the rehybridization of $\pi$ and $\sigma$ orbitals. The significant changes of electronic structure are proved to be a measure for the mean diameter of the macroscopic amounts of SWNTs.

KEYWORDS: Carbon nanotubes; X-ray emission spectroscopy; Quantum confinement.

*Authors to whom correspondence should be addressed.

E-mail address: jguo@lbl.gov   (Guo); wuzy@mail.ihep.ac.cn (Wu)

Carbon nanotubes (CNTs) have attracted much attention due to their variety of potential applications.[1] Extensive research efforts have focused on the electronic structure.[2] The common model is graphene zone-folding, which imposes periodical boundary conditions on the 2D energy dispersion of graphene.[3] However, such a model neglects the finite curvature of tube wall. Carbon atom has 6 electrons that occupy $1s$, $2s$, and $2p$ atomic orbitals. The $2s$ and $2p$ atomic orbitals can readily mix to form $sp^2$ and $sp^3$ hybrids. In both graphite and CNTs the hybridization is $sp^2$ type. In graphite the $\pi$ orbitals are perpendicular to the graphene plane, while in CNTs the $\pi$ orbitals are oriented along the normal to nanotube surface and thus are not parallel to each other due to the surface bending.[4] They mix with $\sigma$ orbitals of the neighboring sites, and such mixing would affect the band structure of CNTs. Optical absorption spectroscopy and STM[5-7] have shown the electronic structure changes near Fermi level along with the curvature for single nanotube. The curvature effect opens a small bandgap for metallic nanotubes.[5] A semiconductor tube has a bandgap inversely proportional to its diameter $d$ while the chiral metallic and zigzag metallic tube are predicted to have narrow-gap scaling by $1/d^2$.[5-7] The chemical reactivity showed dependence on the tube diameter or curvature.[8] Although the electronic structure near Fermi level has been widely investigated, the curvature effect on the whole band structure and especially the $\sigma$ bands is still largely unknown. In this letter we show the band structure changes in both $\pi$ and $\sigma$ bands using soft-x-ray absorption (XAS) and emission spectroscopy (XES), and the results indicate that the rehybridization of $\pi$ and $\sigma$ orbitals affects both $\pi$ and $\sigma$ bands in SWNTs.

XAS probes the unoccupied density of states (DOS) and XES probes the occupied DOS.[9] In addition to the inherent elemental selectivity of x-ray spectra, resonant excitation allows separation of features that pertain to different elements or same element in different chemical environments.[10] Today the method is frequently applied in research fields ranging from atomic and molecular physics to materials science.[11] The study of the quantum confinement of SWNTs demonstrates the important potential for investigating the electronic structure of SWNTs.

The XAS and XES experiments were performed at BL7 of ALS[12] and the XES spectra were collected using a Nordgren-type spectrometer.[13] The resolution was set to 0.2 eV and 0.3 eV for XAS and XES measurements, respectively. The resolution of the spectrometer was set to 0.3 eV. The incident angle was 20° to sample surface in order to minimize the self-absorption effect with the spectrometer orthogonal to incoming photon beam. The XAS spectra were recorded using total electron yield (TEY) mode with the energy scale calibrated to the $\pi^*$ peak at 285.5 eV in XAS of HOPG.[14]

Three SWNT samples were used in the experiments labeled as SWNT1, SWNT2 and SWNT3. SWNT1 was synthesized by a hydrogen arc discharge method[15] and purified with 90% SWNTs in volume. SWNT2 was prepared by optimal floating chemical vapor deposition (CVD) method[16] and the purified sample contained over 70wt% carbon nanotubes measured by TGA. SWNT3 was purified HiPco SWNTs purchased from Carbon Nanotechnologies Incorporated (CNI)[17] with purity better than 85wt%. SWNT1 has a diameter distribution of 1.78-2.06 nm from Raman spectra with the mean diameter of

1.85 nm. SWNT2 has a diameter distribution of 1.08-1.25 nm from Raman spectra with the mean diameter of 1.15 nm. SWNT3 has a diameter distribution of 0.8-1.2 nm measured by CNI from TEM micrographs with the mean diameter of 1.0 nm. The mean length is about several microns for SWNT1 and SWNT2 and 100 to 1000 nm for SWNT3 based on TEM images.

Fig. 1(a) shows the C $K$-edge XAS spectra of SWNTs of different diameters. All spectra have been normalized to the pre- and post-edges. The absorption features labeled to A and B at 285.5 and 292.5 eV are attributed to the transitions from C 1s level to C-C $\pi^*$ and $\sigma^*$ states, respectively.[18] Along with the increasing diameter of SWNTs, the XAS spectra show no significant angular dependence on the intensity ratio of $\pi^*/\sigma^*$. However, the $\sigma^*$ feature of exciton nature becomes less prominent as the diameter of SWNTs reduces.

Fig. 1(b)-(d) shows XES spectra of SWNTs at excitation energies of 285.5 eV (b), 292.5 eV (c) and 305.4 eV (d), respectively. Six main features (labeled with 1-6) are readily seen. The XES spectra at normal excitation energy have been shown in Fig. 1(d). No significant change is observed from the SWNTs of different diameters. The spectra at normal excitation energy are the sum of different orbitals and symmetries, leading to less symmetry dependence and momentum selectivity. The XES spectra excited on the $\sigma^*$ state shown in Fig. 1(c) show no significant difference.

The big changes appear in Fig. 1(b), where the resonant XES spectra of SWNTs of different diameters at $\pi^*$ excitation energy of 285.5 eV are displayed. All emission peaks show strong intensity variations upon SWNT's diameter. In addition, a shift to lower

energy for peak1 and peak2 near Fermi level is clearly seen when the diameter decreases from SWNT1 (1.85 nm) to SWNT3 (1.0 nm).

To clarify the changes in band structure, Fig. 2 shows the curve fitting results in (a) for the energy positions of peak1 and peak2 and in (b) for the intensity ratio of peak5/peak4. The pictures on top of both Fig. 2(a) and (b) show the peak fitting curves for the corresponding peaks (SWNT2 as an example). The inset on top of Fig. 2(a) also shows the whole XES spectrum with elastic peak. In Fig. 2(a) the peak positions of peak1 and peak2 shift to lower energy when the SWNT's diameter decreases. Resonant inelastic x-ray scattering (RIXS) theory predicts that the control over excitation energy allows one to select the crystal momentum of the photoelectron's final state in the conduction band.[19] The excitation energy of 285.5 eV is just above Fermi level and the corresponding emission spectra show the band structure near $K$ point.[9] According to previous reports,[20] core hole effects will contribute to the $\pi^*$ feature in XAS of graphite. However, The final state in RIXS consists of a hole in the valence band and an electron in the conduction band, so energetic considerations for allowed emission lines imply that *transition process* is largely an interband transition, unaffected by core-hole final-state effects.[21,22] The excitation energy of $\pi^*$ peak can be used to excite the unoccupied electronic structure as shown in theory[22] and experiments.[9,19] The down shift of peak1 and peak2 near Fermi level indicates the lowering of $\pi$ band near $K$ point due to the curvature. For SWNTs the $\pi$ orbitals are not parallel to each other due to the curved surface and will hybridize with the $\sigma$ orbitals. The band structure thus can be modified due to the rehybridization of $\pi$ and $\sigma$

6

orbitals. The lowering of π valence band with the increased curvature (reduced diameter) in the resonant XES spectra indicates the bandgap opening for metallic or semiconductor nanotubes.

The peak intensity evolution in σ band due to the curvature difference is presented in Fig. 2(b). The intensity of peak4 increases while peak5 decreases when the tube curvature increases. Peak4 is even stronger than peak5 when the tube diameter is down to 1.0 nm. From SWNT1 to SWNT3, it shows a dramatic diameter-dependence for the ratio of peak5/peak4. Peak4 and peak5 are σ band features. Prominent intensity changes of peak4/peak5 evident the σ band evolution due to different diameters. Previously, less study has focused on the electronic structure of σ bond because of the constant bond length of σ bond in SWNTs of different diameters. Most of the calculations discussed only the bandgap changes. This result indicates that the σ bond can also be strongly affected by the curvature bending. The possible origins are the bond angle difference or other structural distortion and so further calculation insight would be interesting. It is an intrinsic property of the tubes and the spectral behavior can be used for the characterization of tube diameter. Interestingly, the ratio of peak5/peak4 does not change at different experimental geometry because of σ band properties. Thus it could be an effective way for determining the mean diameters of large amounts of SWNTs.

In regards to the changes near Fermi level, we show in Fig. 3(a) the energy levels of LUMO, HOMO and HOMO-1 for SWNT1, SWNT2, and SWNT3 derived from the XAS and XES spectra. To simplify the analysis process, we choose the lowest peak in XAS (π*)

as LUMO, the highest peak in XES (peak1) as HOMO and the next peak for HOMO-1. The LUMO shows nearly no energy shift for different SWNTs while the HOMO and HOMO-1 show a shift to lower energy with decreased diameter. The energy difference between LUMO and HOMO reflects the bandgap (Eg) of SWNTs and thus Eg (LUMO-HOMO) vs $d$ (diameter) can reflect the change for SWNTs with different diameters. Fig. 3(b) shows the energy difference for the three SWNTs samples and the corresponding curve fitting. The fitting result shows a relation between bandgap and SWNT's diameter with $Eg=0.0038/(d-0.85)^2+2.111$. The increased curvature alters the $\pi$-electron wave function and changes the bandgap or spike like density of states due to the van Hove singularity.

In conclusion we have investigated the quantum confinement of SWNTs on bonding and rehydridization of $\pi$ and $\sigma$ orbitals and bandgap change by using resonant x-ray emission spectroscopy. At the excitation energy of 285.5 eV ($\pi^*$), the emission spectral features change drastically due to the surface bending of SWNTs. The changes can be related to the $\pi$ and $\sigma$ band structure evolution near $K$ point. The results indicate that the rehybridization of $\pi$ and $\sigma$ orbitals has changed both $\pi$ and $\sigma$ bonds in SWNTs, and elude a possible way of determinning the mean tube diameter for macroscopic amounts of SWNTs.

## References

[1]   R. H. Baughman et al., Science **297**, 787 (2002).

[2]   M. Burghard, Surface Science Reports **58**, 1 (2005).

[3]   R. Saito et al., Appl. Phys. Lett. **60**, 2204 (1992).

[4]   P. Lambin, Comptes Rendus Physique **4**, 1009 (2003).

[5]   C. L. Kane, E. J. Mele, Phys. Rev. Lett. **78**, 1932 (1997).

[6]   Y. J. W. Ding et al., J. Phys. Condens. Matter **15**, L439 (2003).

[7]   T. W. Odom et al., Nature **391**, 62 (1998).

[8]   S. Park et al., Nano Lett. **3**, 1273 (2003).

[9]   P. Skytt et al., Phys. Rev. B **50**, 10457 (1994).

[10] J.-H. Guo et al., Phys. Rev. Lett. **91**, 157401 (2003).

[11] J.-H. Guo, Int. J. Nanotechnology, **1-2**, 193-225 (2004).

[12] T. Warwick et al., Rev. Sci. Instrum. **66**, 2037 (1995).

[13] J. Nordgren et al., Rev. Sci. Instrum. **60**, 1690 (1989).

[14] L.J. Terminello et al., Chem. Phys. Lett. **182**, 491 (1991).

[15] C. Liu et al., Carbon **37**, 1865 (1999).

[16] L. Song et al., Adv. Mater. **16**, 1529 (2004).

[17] P. Nikolaev et al., Chem. Phys. Lett. **313**, 91 (1999).

[18] A. Kuznetsova et al., J. Am. Chem. Soc. **123**, 10699 (2001).

[19] J. A. Carlisle et al., Phys. Rev. Lett. **74**, 1234 (1995).

[20] P. A. Brühwiler et al., Phys. Rev. Lett. **74**, 614 (1995).
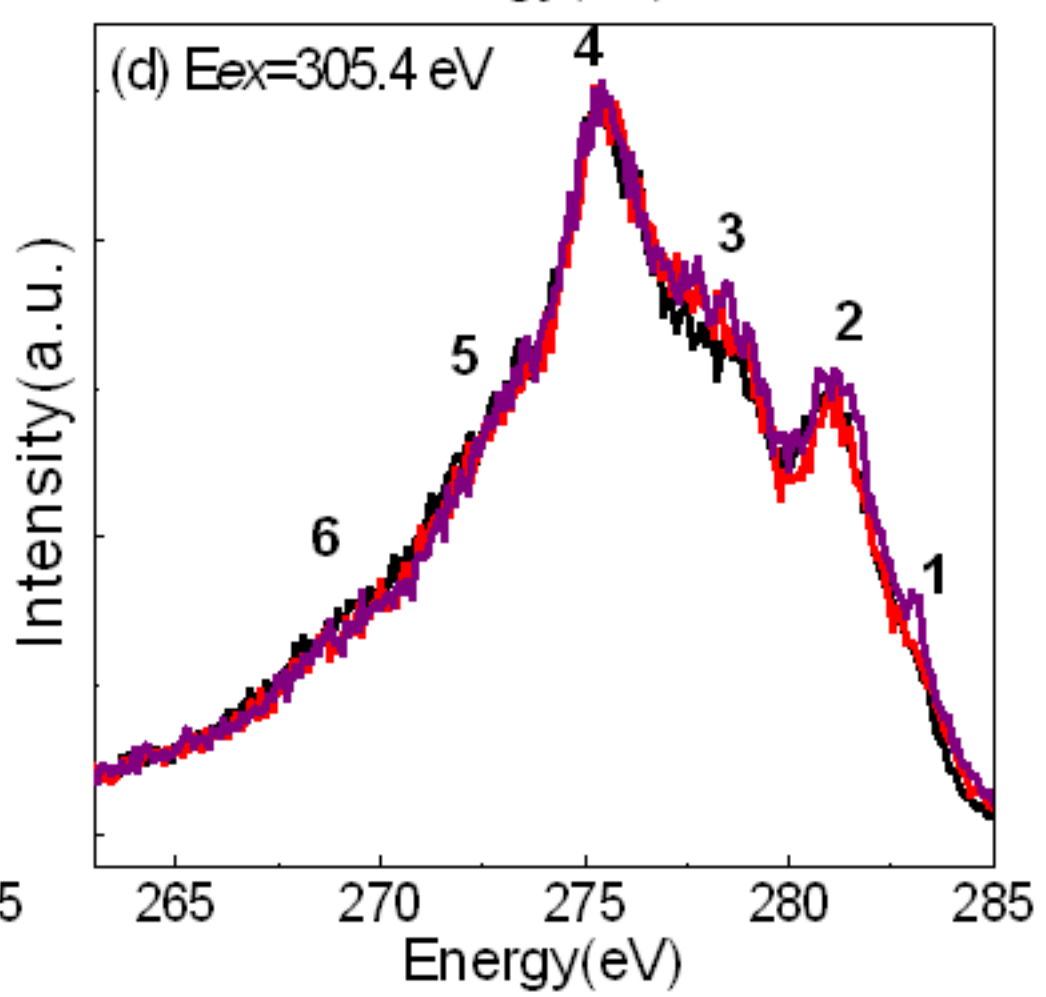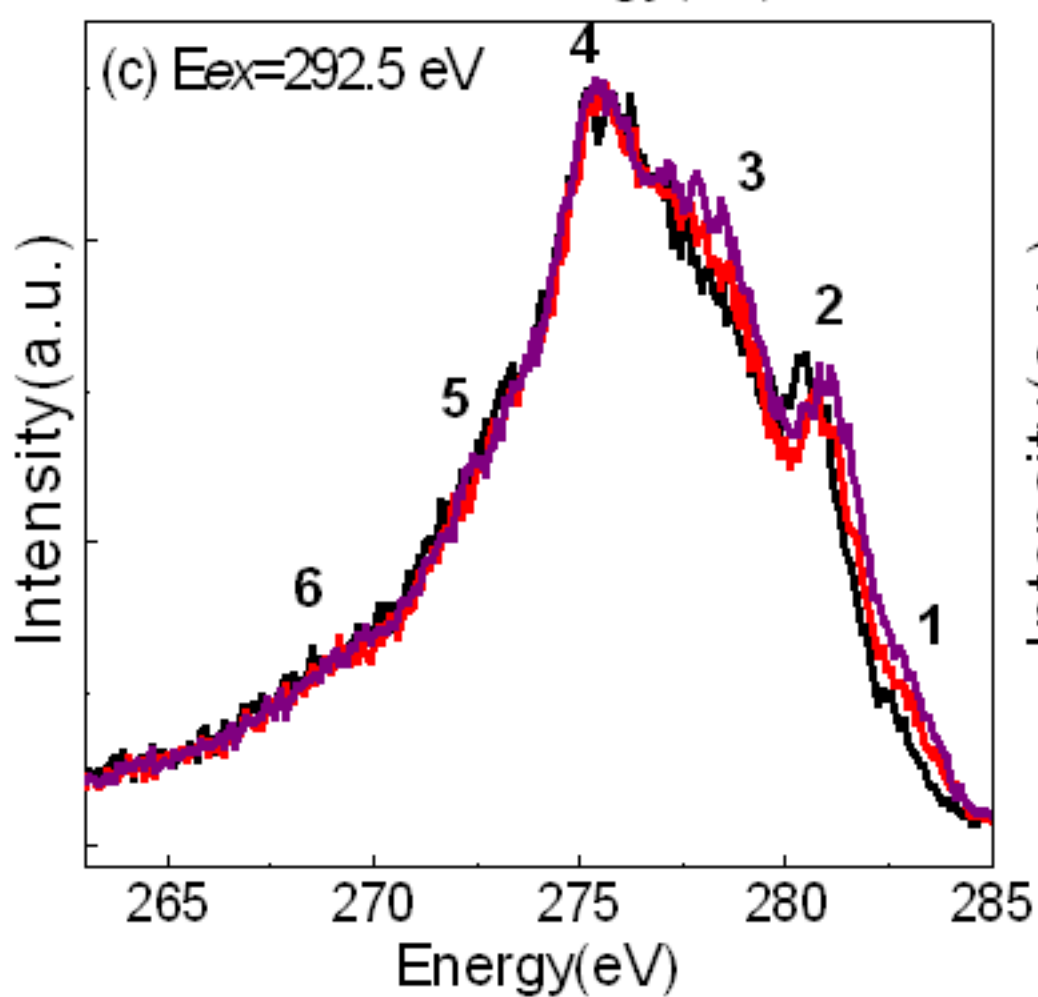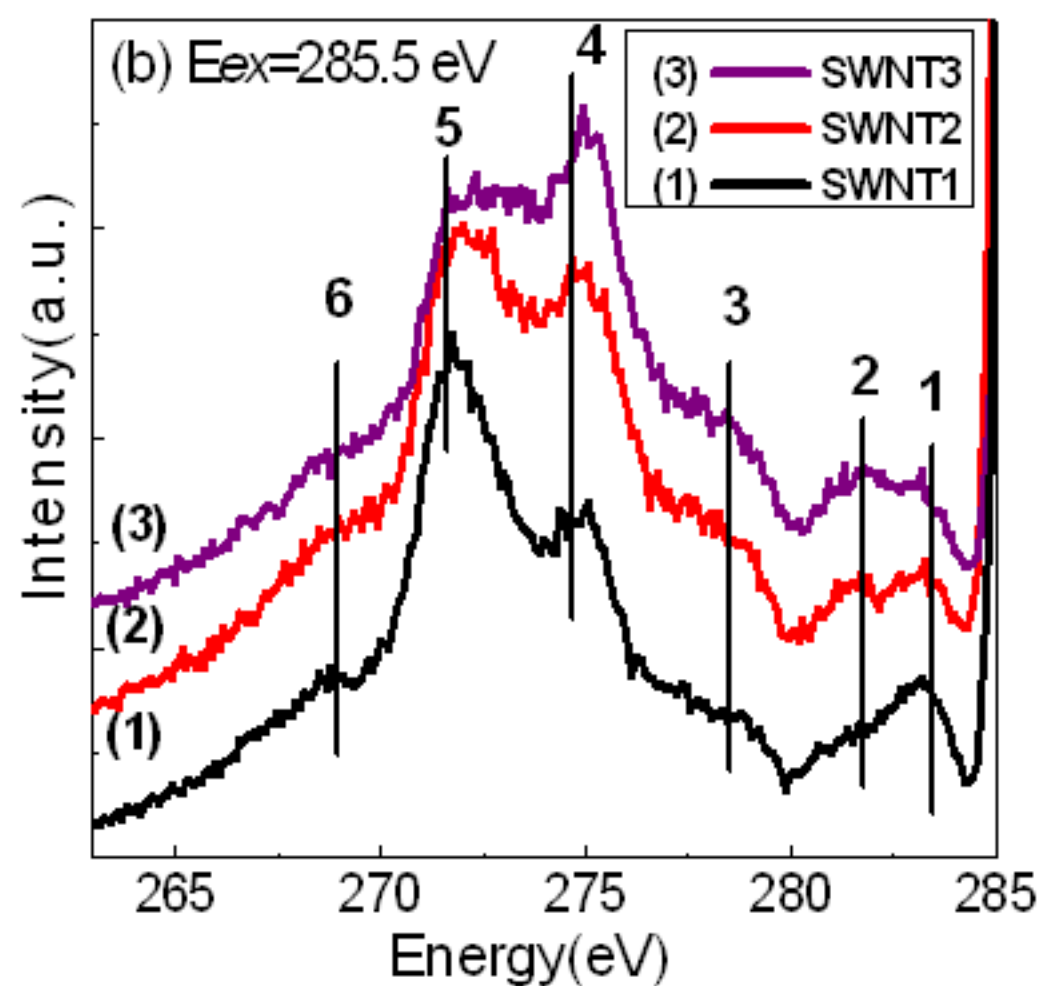
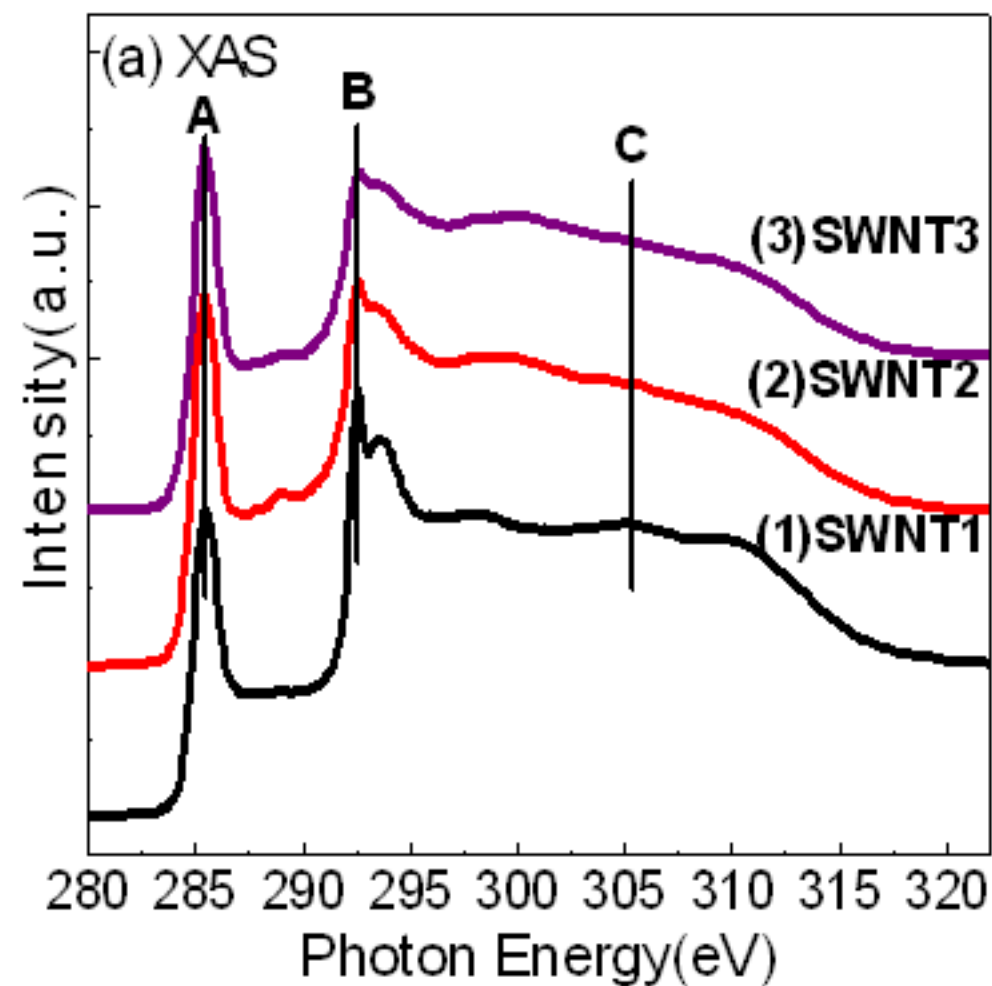[21] J. A. Carlisle et al., Phys. Rev. Lett. **76**, 1762 (1996).

[22] Y. Ma, Phys. Rev. B **49**, 5799 (1994).

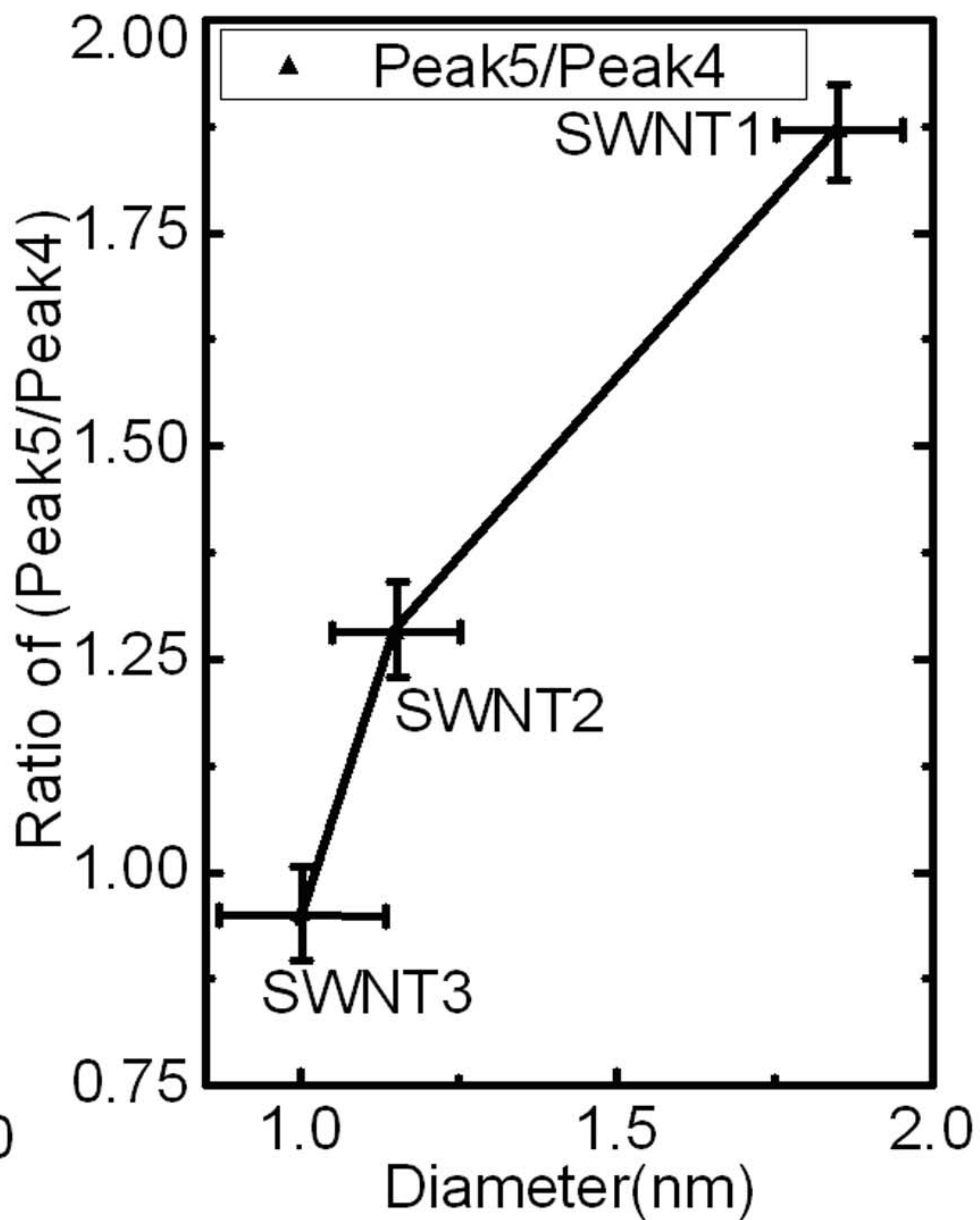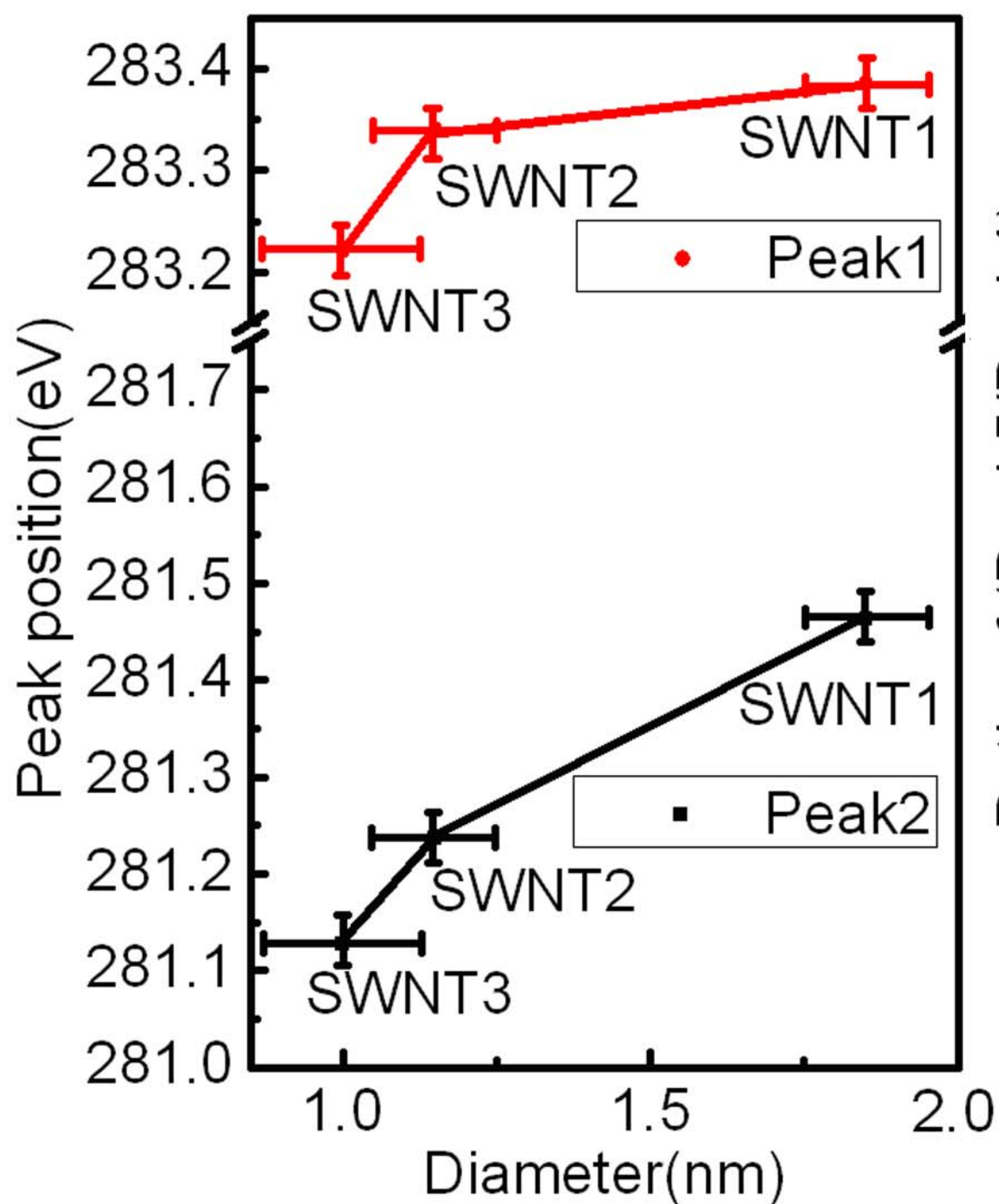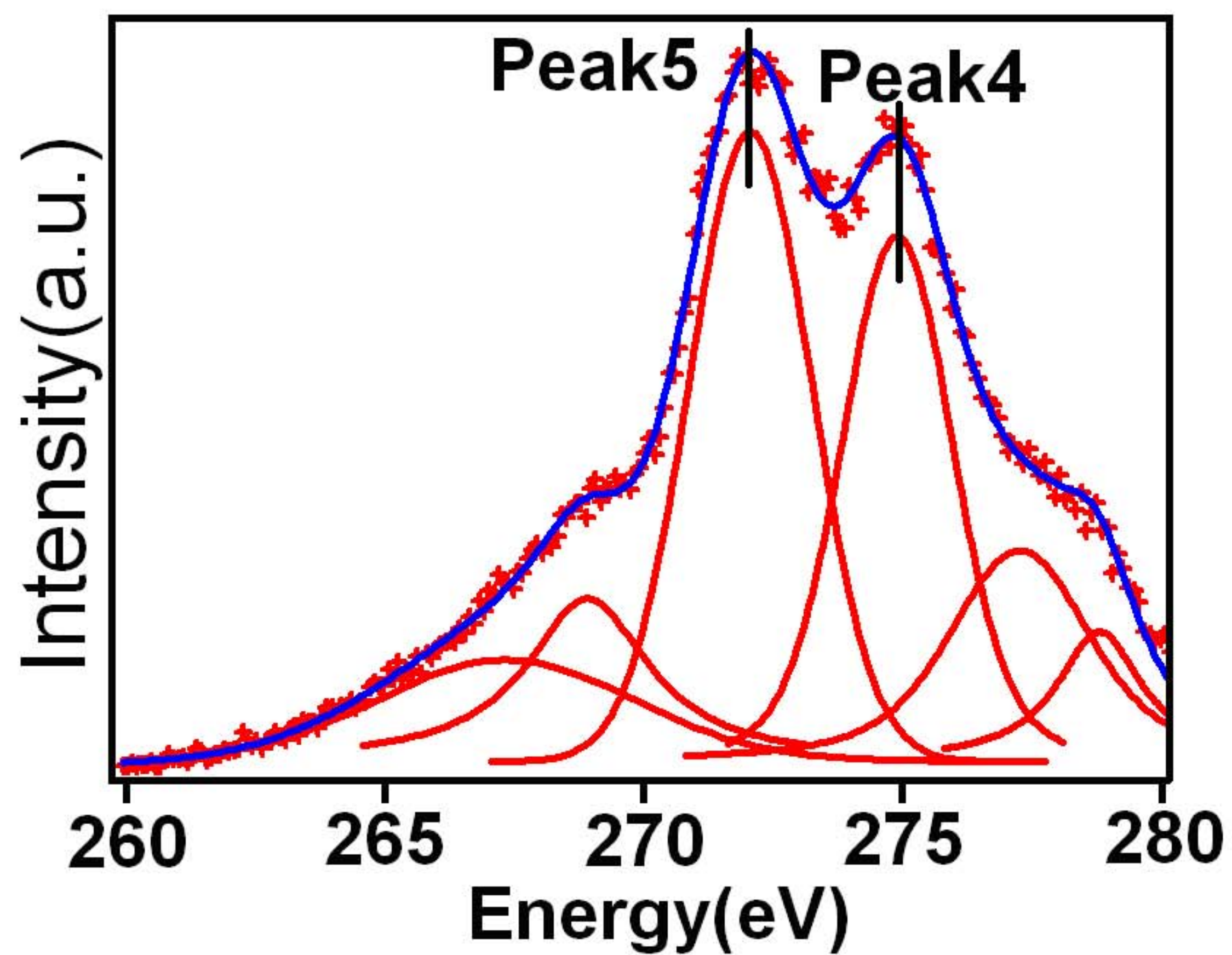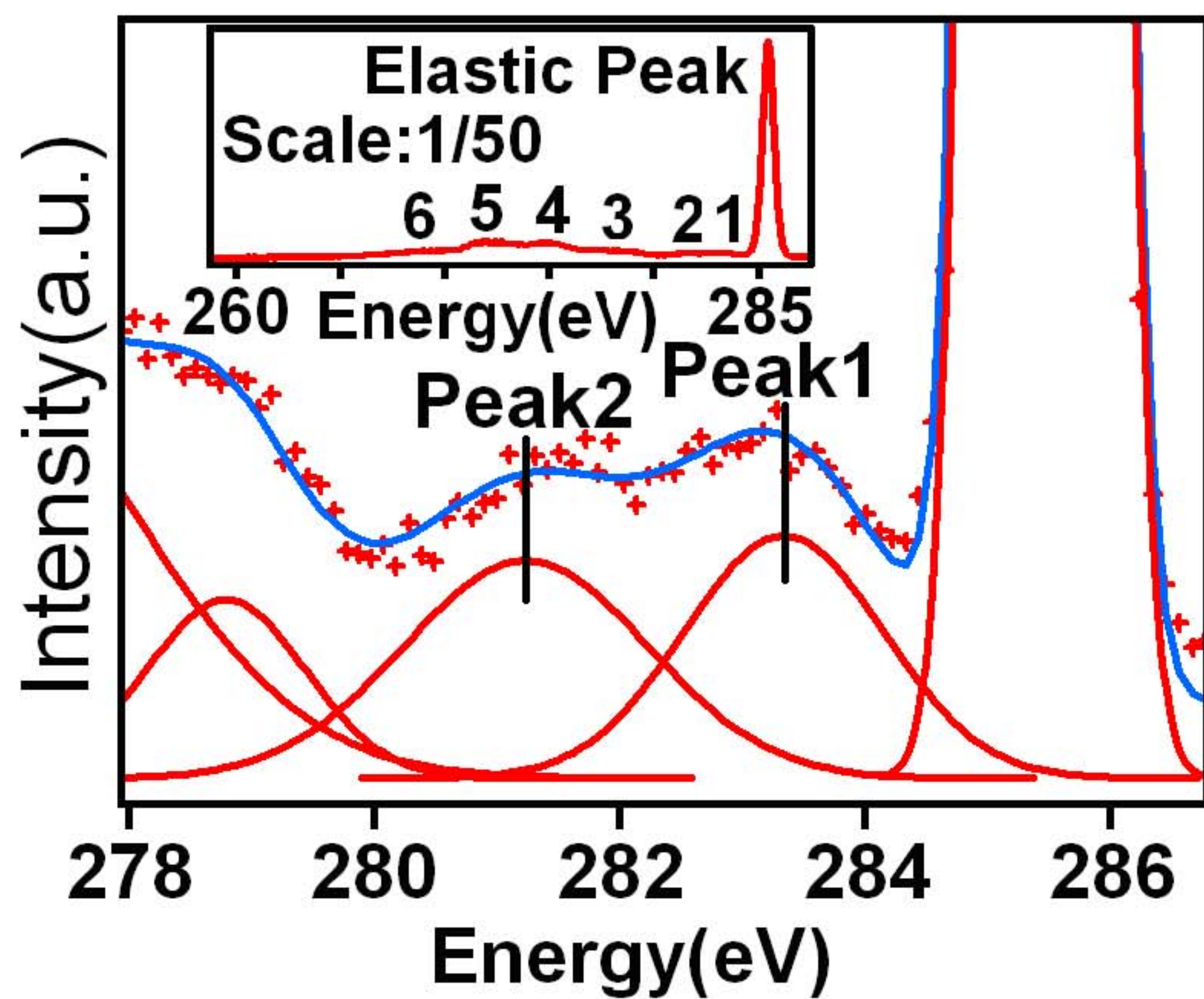**Figure captions:**

Fig. 1: C *K*-edge absorption spectra and emission spectra of SWNT1, SWNT2 and SWNT3. (a) C *K*-edge absorption spectra (XAS) and C *K*-edge emission spectra at different excitation energies of 285.5 eV (b), 292.5 eV (c) and 305.4 eV (d).

Fig. 2: (a) The energy positions of peak1 and peak2, and (b) the intensity ratio of peak5/peak4 at the excitation energy of 285.5 eV vs the diameter of SWNT1, SWNT2 and SWNT3. The panels on top of both (a) and (b) show the peak fitting curves for the corresponding peaks (SWNT2 as an example).
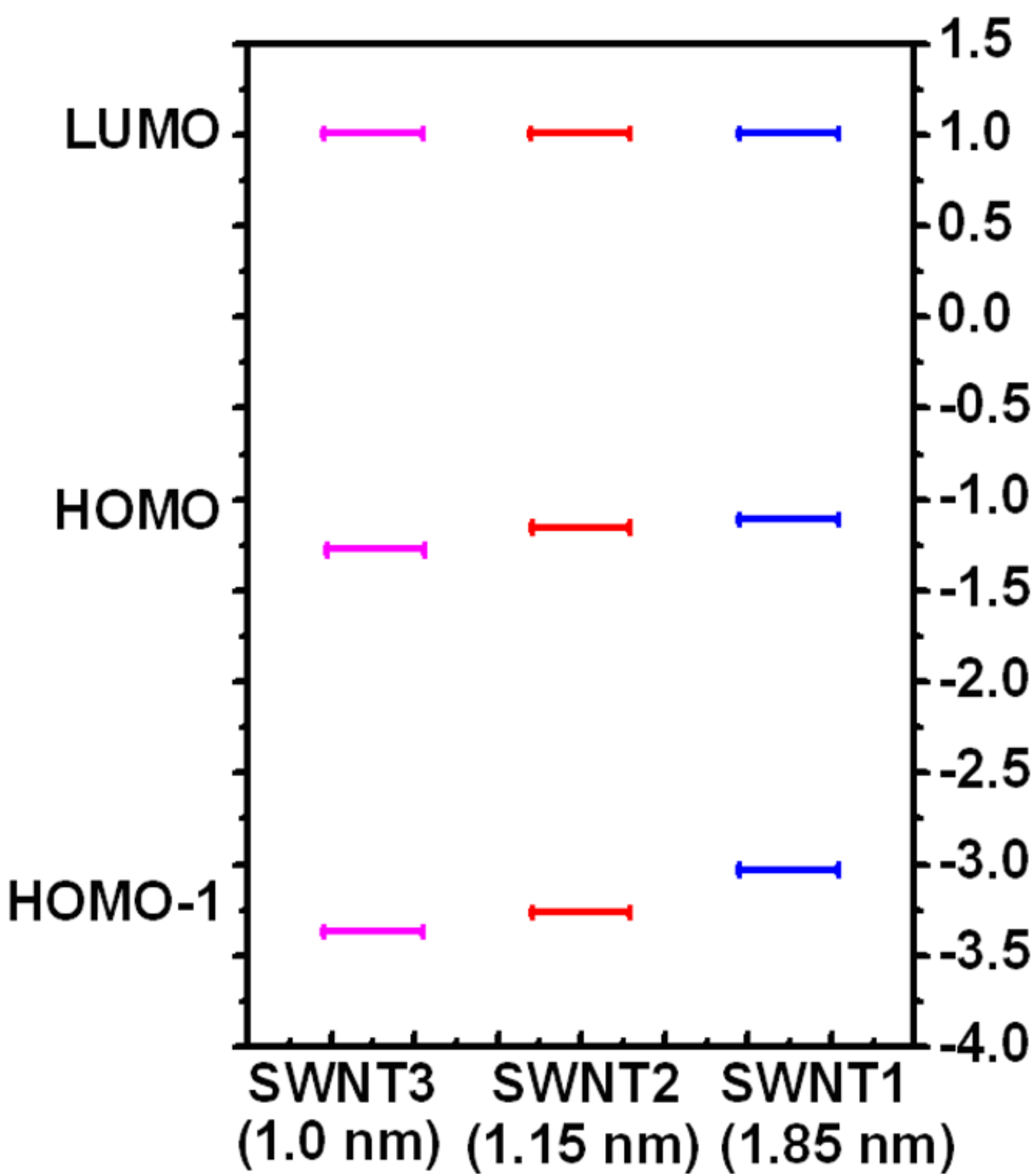
Fig. 3: (a) The energy levels of LUMO, HOMO and HOMO-1 for SWNT1, SWNT2, and SWNT3. (b) The energy difference between LUMO and HOMO for three samples and the fitting curve.
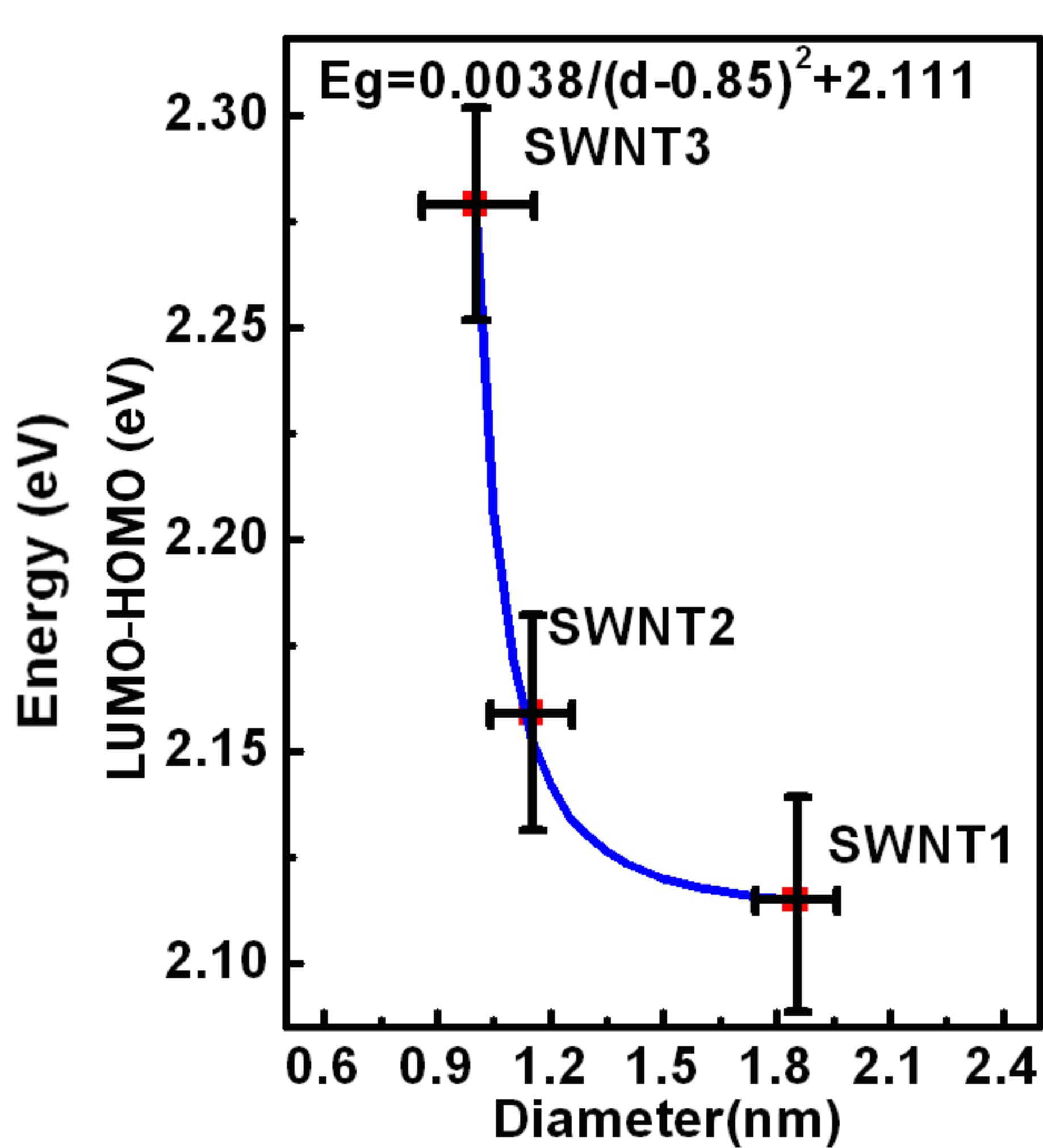
(a) XAS

A
B
C

(3) SWNT3
(2) SWNT2
(1) SWNT1

Intensity(a.u.)

Photon Energy(eV)

(b) Eex=285.5 eV

(3) SWNT3
(2) SWNT2
(1) SWNT1

6
5
4
3
2
1

(3)
(2)
(1)

Intensity(a.u.)

Energy(eV)

(c) Eex=292.5 eV

4
3
2
5
6
1

Intensity(a.u.)

Energy(eV)

(d) Eex=305.4 eV

4
3
2
5
6
1

Intensity(a.u.)

Energy(eV)

(a)

(b)

(a)

(b)

$Eg = 0.0038/(d-0.85)^2 + 2.111$